

# GENERATING ELECTRICITY AT A BREAKWATER IN A MODERATE WAVE CLIMATE

Joris Schoolderman<sup>1</sup>, Bas Reedijk<sup>2</sup>, Han Vrijling<sup>3</sup>,  
Wilfred Molenaar<sup>3</sup>, Erik ten Oever<sup>2</sup> and Marcel Zijlema<sup>3</sup>

A new concept for wave energy conversion is examined as a proof of concept for generating electricity in a moderate wave climate while being integrated in a caisson breakwater. Physical model testing is performed to analyse the preliminary efficiency of the device and to identify areas of improvement. The resulting device is calculated for two sample locations in order to gain an understanding of its feasibility. Recommendations are made for continued research and possible improvements of the design.

*Keywords: wave energy converter; caisson breakwater; renewable energy*

## INTRODUCTION

Waves offer a vast renewable energy source. In response to the desire to increase utilisation of renewable energy sources, many wave energy converters (WECs) are currently under development. Some have built prototypes or have even begun pilot testing. Unfortunately, the energy from waves has proven difficult to capture in an efficient and cost effective manner.

This paper, based on recent research (Schoolderman 2009), proposes a new concept for wave energy conversion. The objective of this research was to create and test a new wave energy converter that can be integrated within a breakwater. In the new concept the primary function of the device will remain the protection of the harbour. In doing this, a WEC has been designed which is capable of adding a revenue generation function to a breakwater while adding cost sharing benefits due to integration.

Economic expansion continuously requires additional breakwater construction and existing breakwater reparation. During these construction activities it could be possible to include the WEC proposed in this report for a relatively low price considering the breakwater would be built regardless of the inclusion of a WEC.

## Improvement Points of Existing Concepts

Current WECs are designed to generate the maximum possible electricity from waves and are placed in very energetic wave climates to maximise electrical production. Wave energy increases exponentially with height which means, although more energy can be produced, the device itself must also be designed extremely robust. This is particularly the case to survive storms.

Many WECs are designed to be offshore because of the availability of highly energetic wave climates. This requires expensive support and anchoring structures due to the extreme loading conditions and an extensive connection to the electrical grid. Existing WECs are optimised for these highly energetic wave climates and would not function effectively relative to cost in moderate wave climates (i.e. smaller waves).

Additionally, many current WECs are quite complex with many vulnerable and moving parts (i.e. hydraulic pistons). In order to increase the life expectancy of a WEC and decrease overall costs including maintenance, it is beneficial to reduce the amount of these vulnerable components.

## Starting Points for New Concept

The following starting points were established for this project based on the identified improvement points:

- Integration in caisson breakwater:

The primary function of the structure will continue to be the protection of the harbour. Generating electricity is a secondary function. Therefore, the structure will remain a fixed concrete structure. Due to the proximity of breakwaters to the coast a less extensive connection to the electrical grid can be realised.

---

<sup>1</sup> Witteveen+Bos Consulting engineers, P.O. Box 2397, 3000 CJ Rotterdam, The Netherlands

<sup>2</sup> Delta Marine Consultants, P.O. Box 268, 2800 AG Gouda, The Netherlands

<sup>3</sup> Delft University of Technology, Faculty Civil Engineering & Geosciences, Stevinweg 1, 2628 CN Delft, The Netherlands

- Conversion from moderate daily wave climate:

The device is intended to be used in regions where the normal daily wave climate is  $H_{s,daily} \approx 0.5 - 1.5$  m and  $T_p \approx 5 - 10$  s. This range was chosen because these smaller waves are found to occur at many locations. Also, many current WECs favour larger and more energetic waves for the sole purpose of generating electricity leaving this range open for development.

- Minimise moving parts:

Minimising the number of components with moving parts will decrease the maintenance required. Components that do consist of moving parts (such as turbines) will be placed in an area out of direct contact with wave action. This will also help ensure that maintenance can be performed in an area away from waves.

The three main starting points all ensure robustness of the device. A breakwater is specifically designed to survive storms and the WEC inside can remain protected. Also, areas with a more moderate daily wave climate often also have less severe storm conditions requiring less over-dimensioning. Finally, moving parts are often vulnerable to damage. Omitting as many as possible can enhance the device robustness.

### PRESSURE CONCEPT

Several alternative concepts were investigated as a result of the starting points. Out of this initial research the pressure concept was chosen to model test and analyse.

In the pressure concept, dynamic wave pressure is exerted on an underwater opening (ramp entrance) in the caisson face causing the flow of water into a ramp with a gradual constriction. The constriction increases the pressure allowing the water to enter a storage basin at a to-be-determined optimal elevation above mean water level (MWL) at the ramp exit. The water is returned to the sea at the rear of the structure through a turbine. An overall impression of the concept is depicted in Figure 1.

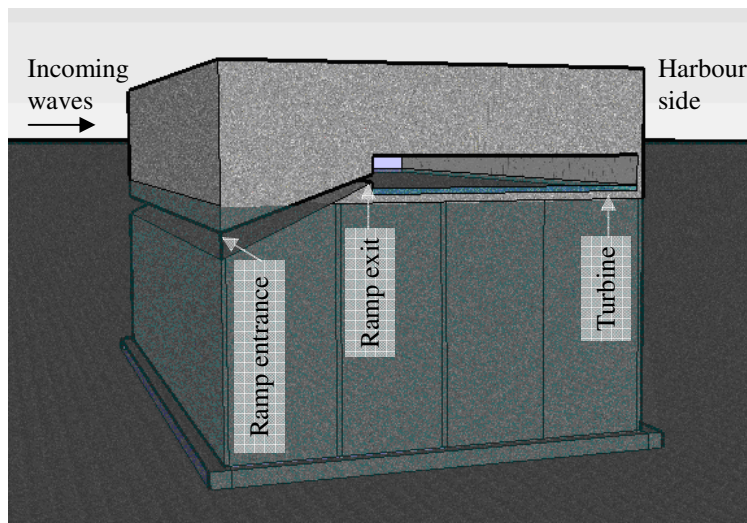


Figure 1. Impression of pressure concept, cross-section of caisson element

In the impression in Figure 1, waves approach the structure from the left and the protected harbour is on the right. Also, the constricting ramp and the internal basin can be seen in the cross-section. At the rear of the structure (harbour side) the water in the basin will flow back to the sea.

### MODEL TESTING

To observe and analyse the practicality and efficiency of this concept, physical model testing was performed at the wave flume operated by Delta Marine Consultants. A plywood model was constructed at a scale of 1:25 in order to test the following:

- Effect of varying wave climate
- Optimum opening ratio
- Effect of crest freeboard

It is important for a WEC to function in a wide range of conditions. However, this particular WEC focuses on a specific moderate daily wave climate. Therefore, the climate set forth in the starting points was the testing range. The range  $H_s = 0.5 - 1.5$  m and  $T_p = 5 - 10$  s was used, resulting in a model scale wave climate of  $H_s = 2 - 6$  cm and  $T_p = 1 - 2$  s.

The opening ratio (OR) is the ratio between the opening size of the ramp entrance (lower underwater side of ramp) and the ramp exit (upper side of ramp). In order to select the optimum opening ratio, three different ratios were examined through means of constructing one model with three ramps. The ramps were connected to different internal basins so they could be monitored independently.

Due to tide and sea level rise the crest freeboard can vary. In order to examine the effect of this the model was tested using two water depths, distinguished as Series 1 and 2.

The model was constructed as shown in Figure 2 and placed on top of a 1/50 slope foreshore which came to a height of approximately 39 cm. The water level indicated is for the Series 1 tests.

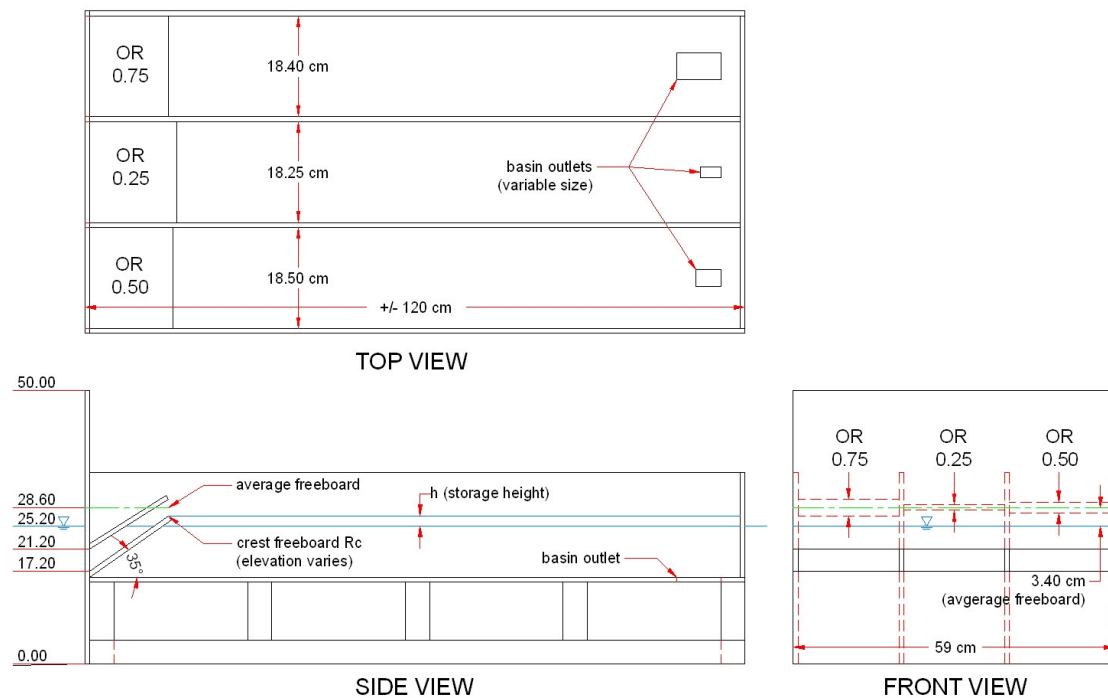


Figure 2. Sketch of model (elevations in cm above foreshore platform)

The model was created such that the three ramps have the same average freeboard. This is best visualised in the front view of Figure 2 where the vertical midpoint of the opening is 3.40 cm above MWL for all ramps in Series 1. Because the ramp exit sizes vary the crest freeboard is at a different elevation for each ramp.

The ramps were each built with a 4 cm high ramp entrance (underwater opening) and a width equal to the width of the basins. The top of the ramp entrance is at a depth of 4 cm below Series 1 MWL and the average freeboard is  $\pm 3.40$  cm above Series 1 MWL. The constructed ramp widths were 18.25, 18.50 and 18.40 cm for opening ratios of 0.25, 0.50 and 0.75, respectively.

### Test Setup

Figure 3 shows an overview of the two-dimensional wave flume and the Edinburgh Designs piston wave generator. The wave flume is 25.0 m long, 0.6 m wide, and 1.0 m high. The maximum possible water depth is 0.7 m and  $H_{max}$  is 0.3 m depending on the water depth. At the right of Figure 4 the placement of the model can be seen.



Figure 3. Overview wave flume and wave generator

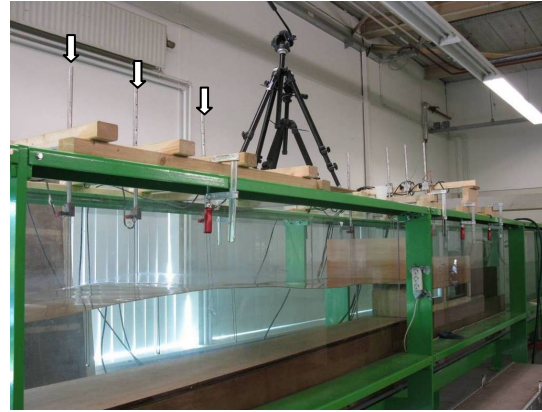


Figure 4. Model in flume and depth gauge array

In total, eight depth gauges were used. Three gauges were set up in an array in front of the model (Figure 4), one gauge directly in front (Figure 5) and at the rear of the model (Figure 6), and one gauge was placed in the centre of each of the three internal basins (Figure 7). The arrows in the figures indicate the locations of the gauges.

The array of three instruments in Figure 4 allows the ability to distinguish between incident and reflected waves. The software (WaveLab 3.04) uses the measurements from this array to calculate incident and reflected wave characteristics including, amongst others,  $H_{m0}$ , reflection coefficient and incoming wave power. For the purpose of this study  $H_{m0} = H_s$ .



Figure 5. Depth gauge in front of model

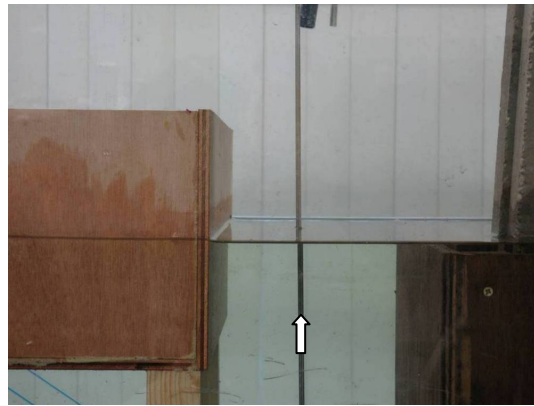


Figure 6. Depth gauge behind model

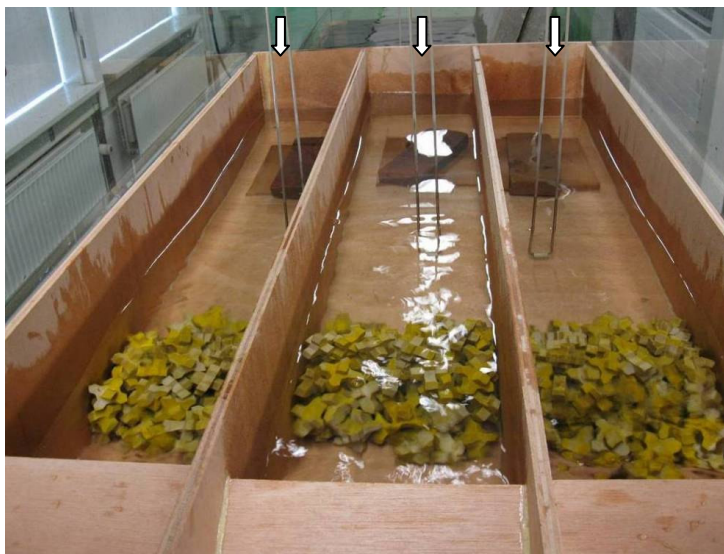


Figure 7. Depth gauges in individual basins

The yellow elements within the individual basins in Figure 7 were added during testing because it was found that spillback occurred. Spillback is when waves entering the internal basin through the ramp continue propagating through the basin, reflect off the rear wall and exit through the ramp again. In order to reduce spillback the elements were placed to dissipate the incoming wave energy.

The depth gauges located at the centre of the three individual basins (Figure 7) continuously measure the height of water in each of the basins. Comparing these measurements to the still water level in the flume measured at the rear of the model (Figure 6) allows the flow of water through the basin outlets to be determined. The quantity of water passing through the basin outlets is equivalent to the effective inflow of water through the ramps.

### Testing Program

In order to test the various parameters of importance twelve tests were performed. Six tests (Series 1) were performed with a water depth of 25.20 cm directly in front of the model, a significant wave height of approximately 2 cm, 4 cm and 6 cm and a peak wave period of 1 s and 2 s. An additional six tests (Series 2) were performed with a water depth of 26.35 cm directly in front of the model, a significant wave height of approximately 2 cm, 4 cm and 6 cm and a peak wave period of 1 s and 2 s.

Testing of the effect of the varying opening sizes and ratios occurs because during each test three different openings are present. Also, raising the water elevation by 1.15 cm reduces the average freeboard and ensures varying crest freeboard is also tested. Wave characteristics, water depth and crest freeboard per ramp were measured during the testing. The actual wave conditions and water depths used for the testing are presented in Table 1.

Table 1. Sequence of model tests									
Series 1 tests: water depth = 25.20 cm average freeboard = $\pm 3.40$ cm					Series 2 tests: water depth = 26.35 cm average freeboard = $\pm 2.25$ cm				
Test 1		Test 2			Test 7		Test 8		
$H_s$ (2 cm)	2.038 cm	$H_s$ (2 cm)	2.042 cm		$H_s$ (2 cm)	2.072 cm	$H_s$ (2 cm)	2.081 cm	
$T_p$ (2 s)	2.065 s	$T_p$ (1 s)	1.016 s		$T_p$ (2 s)	2.065 s	$T_p$ (1 s)	0.970 s	
Test 3		Test 4			Test 9		Test 10		
$H_s$ (4 cm)	4.324 cm	$H_s$ (4 cm)	4.090 cm		$H_s$ (4 cm)	4.384 cm	$H_s$ (4 cm)	4.169 cm	
$T_p$ (2 s)	2.065 s	$T_p$ (1 s)	1.016 s		$T_p$ (2 s)	2.065 s	$T_p$ (1 s)	1.016 s	
Test 5		Test 6			Test 11		Test 12		
$H_s$ (6 cm)	6.696 cm	$H_s$ (6 cm)	6.193 cm		$H_s$ (6 cm)	6.783 cm	$H_s$ (6 cm)	6.298 cm	
$T_p$ (2 s)	2.065 s	$T_p$ (1 s)	1.016 s		$T_p$ (2 s)	2.065 s	$T_p$ (1 s)	1.016 s	

The wave information presented in Table 1 was generated in the wave flume according to the JONSWAP spectrum. Tests were run for approximately 10 minutes (when  $T_p = 1$  s) or 20 minutes (when  $T_p = 2$  s) to ensure that a minimum of 500 waves approached the model and a reasonable representation of the significant wave height is present.

### Calibration

To ensure accurate calculation of results, calibration tests were performed for each basin and water level. The purpose of calibration was to discover the values of the coefficients which allow the calculation of volume of water passing through the outlets based on the head difference. The equation used for calibration as well as the evaluation of the model tests is presented in Eq. 1 where  $V$  is the volume of water,  $f_i$  is the to-be-defined basin outlet coefficient,  $A_{out}$  is the basin outlet area,  $h(t)$  is a function of the head difference and  $g$  is gravity.

$$V = f_i \cdot \int_{t_1}^{t_2} A_{out} \sqrt{2 \cdot h(t) \cdot g} \cdot dt \quad (1)$$

Eq. 1 determines the volume of water discharged through the basin outlet. This is equivalent to the inflow of water through the ramps.



The basin outlets (the location of discharge from the basins back to the flume) were prepared by subjecting the model to the waves expected to have the highest overtopping (mainly  $H_s = 6$  cm at  $T_p = 1 - 2$  s) and making the basin outlet large enough until spillback appeared to no longer occur. The basin outlet areas were kept constant for the remainder of the tests. The areas used are presented in Table 2.

Table 2. Basin outlet areas ( $A_{out}$ )		
Opening Ratio	Outlet Area ( $cm^2$ )	
	Series 1	Series 2
0.25	4.35	7.40
0.50	11.60	13.92
0.75	21.78	40.59

After the basin outlet areas were established the calibration tests were performed. 10 litres of water was emptied into each internal basin while the water levels were monitored and no waves were present in the flume. Data was recorded on the height of water inside each basin and behind the model. These values were corrected to the same reference level. Using these two corrected values, the head difference between basin and flume water level could be calculated.

It became apparent that the water levels never reached equilibrium between the basin and behind the model during the measurements. The measurements were stopped too early because the drainage of water took much longer than expected and the changing water level was no longer distinguishable. However, it was possible to improvise data for this time period because it was known no additional water was added to the system and it acts as a free flowing basin. The remaining required data could be generated using Eq. 1. At this stage the coefficient is assumed and will be corrected through iteration.

The improvised data fit the trend of the available data very well and is a reasonable correction. An example of this is shown for OR=0.50 Series 1 in Figure 8. It should be noted the fluctuations in approximately the first 45 seconds of measurement (differs per calibration test) were caused by small vibrations and sensitivities and were negated from subsequent calculations. The net discharge over this period is negligible.

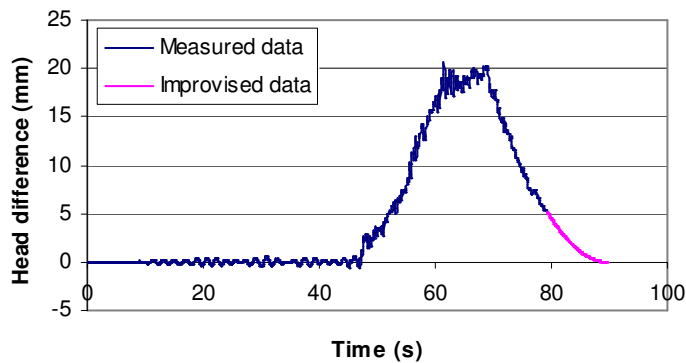


Figure 8. OR=0.50 Series 1 head difference internal basin and behind model

With a full plot of the head difference the volume of water discharged through the basin outlets can be calculated. This is also done using Eq. 1; however, the coefficient is unknown and cannot be determined from a list of standard orifice coefficients. The coefficient is determined through iteration, so that the known volume of water entered into the system (10 litres) becomes the total volume of water measured to exit through the basin outlet. A sample solution is presented in Figure 9.

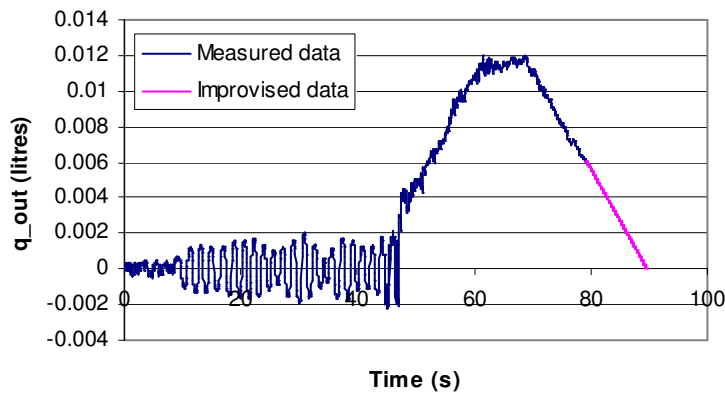


Figure 9. OR=0.50 Series 1 flow of water through basin outlet

In total six coefficients were determined; one for each opening ratio and series of tests. The coefficients obtained from the calibration tests are displayed in Table 3.

Table 3. Values for coefficient $f_i$		
Opening Ratio	Series 1	Series 2
0.25	0.6450	0.5952
0.50	0.5223	0.2888
0.75	0.4144	0.2284

It should be noted the values of the coefficients represent the losses at the basin outlets. Although the discharge of water through the basin outlets was measured it is equivalent to the inflow of water through the ramps. The inflow of water was under investigation and independent of the orifice coefficients. Therefore the orifice losses do not carry over to subsequent calculations.

### Testing Results

Each test was performed as prescribed in Table 1 resulting in the measurement of head differences between each internal basin and the flume still water level. Using Eq. 1 and the coefficients established in Table 3 the flow of water through the basin outlets and the resulting average water capture (AWC) or  $q_{avg}$  are calculated per ramp width.

The power of the captured water was calculated with Eq. 2 where  $\rho$  is water density ( $1000 \text{ kg/m}^3$ ) and  $R_c$  is the crest freeboard.

$$W = q_{avg} \cdot \rho \cdot g \cdot R_c \quad (2)$$

The power that was theoretically available to be converted per ramp can be expressed in watts per linear metre and is compared to the actual power present in the incoming waves (Table 4), resulting in efficiency.

Table 4. Measured incoming wave power			
Test 1	0.3546 W/m <sup>1</sup>	Test 7	0.3558 W/m <sup>1</sup>
Test 2	0.2153 W/m <sup>1</sup>	Test 8	0.2282 W/m <sup>1</sup>
Test 3	1.5790 W/m <sup>1</sup>	Test 9	1.5820 W/m <sup>1</sup>
Test 4	0.8513 W/m <sup>1</sup>	Test 10	0.9034 W/m <sup>1</sup>
Test 5	3.7240 W/m <sup>1</sup>	Test 11	3.7230 W/m <sup>1</sup>
Test 6	1.9640 W/m <sup>1</sup>	Test 12	2.0630 W/m <sup>1</sup>

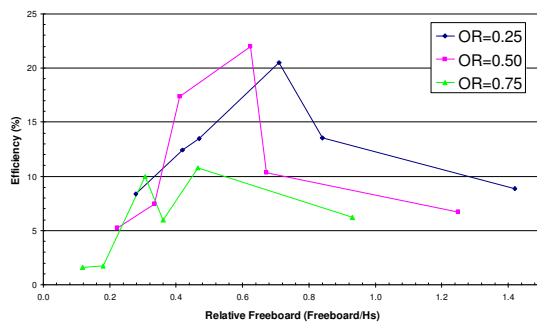
The results of AWC (per ramp width), power (per linear metre) and efficiency are presented in Table 5. It should be noted that, due to inaccuracies caused by an extremely low crest freeboard and resulting high overtopping, the results of Tests 1 and 7 were discarded.

Table 5. Results of model testing										
Series 1 (d=25.20 cm)						Series 2 (d=26.35 cm)				
Wave Condition	OR [-]	R <sub>c</sub> [cm]	AWC [l/s]*	Power [W/m <sup>1</sup> ]	Eff. η [%]	Wave Condition	OR [-]	R <sub>c</sub> [cm]	AWC [l/s]*	Power [W/m <sup>1</sup> ]
<b>Test 1</b>	0.25	2.90	0.022	0.035	9.79	<b>Test 7</b>	0.25	1.75	0.028	0.027
H <sub>s</sub> = 2 cm	0.50	2.55	0.025	0.033	9.43	H <sub>s</sub> = 2 cm	0.50	1.40	0.027	0.020
T <sub>p</sub> = 2 s	0.75	1.90	-0.019	-0.019	-5.33	T <sub>p</sub> = 2 s	0.75	0.75	-0.012	-0.005
<b>Test 2</b>	0.25	2.90	0.012	0.019	8.85	<b>Test 8</b>	0.25	1.75	0.033	0.031
H <sub>s</sub> = 2 cm	0.50	2.55	0.011	0.014	6.70	H <sub>s</sub> = 2 cm	0.50	1.40	0.032	0.024
T <sub>p</sub> = 1 s	0.75	1.90	0.013	0.013	6.22	T <sub>p</sub> = 1 s	0.75	0.75	0.034	0.014
<b>Test 3</b>	0.25	2.90	0.074	0.115	7.28	<b>Test 9</b>	0.25	1.75	0.104	0.098
H <sub>s</sub> = 4 cm	0.50	2.55	0.115	0.156	9.88	H <sub>s</sub> = 4 cm	0.50	1.40	0.091	0.068
T <sub>p</sub> = 2 s	0.75	1.90	0.133	0.135	8.54	T <sub>p</sub> = 2 s	0.75	0.75	0.104	0.042
<b>Test 4</b>	0.25	2.90	0.112	0.174	20.49	<b>Test 10</b>	0.25	1.75	0.119	0.112
H <sub>s</sub> = 4 cm	0.50	2.55	0.138	0.187	22.00	H <sub>s</sub> = 4 cm	0.50	1.40	0.091	0.067
T <sub>p</sub> = 1 s	0.75	1.90	0.090	0.092	10.75	T <sub>p</sub> = 1 s	0.75	0.75	0.039	0.016
<b>Test 5</b>	0.25	2.90	0.148	0.231	6.19	<b>Test 11</b>	0.25	1.75	0.174	0.163
H <sub>s</sub> = 6 cm	0.50	2.55	0.231	0.312	8.37	H <sub>s</sub> = 6 cm	0.50	1.40	0.150	0.111
T <sub>p</sub> = 2 s	0.75	1.90	0.248	0.251	6.75	T <sub>p</sub> = 2 s	0.75	0.75	0.163	0.065
<b>Test 6</b>	0.25	2.90	0.170	0.265	13.48	<b>Test 12</b>	0.25	1.75	0.183	0.172
H <sub>s</sub> = 6 cm	0.50	2.55	0.252	0.341	17.35	H <sub>s</sub> = 6 cm	0.50	1.40	0.146	0.108
T <sub>p</sub> = 1 s	0.75	1.90	0.193	0.196	9.96	T <sub>p</sub> = 1 s	0.75	0.75	0.082	0.033
maximum					22.00	maximum				
minimum					6.19	minimum				

\* per ramp width

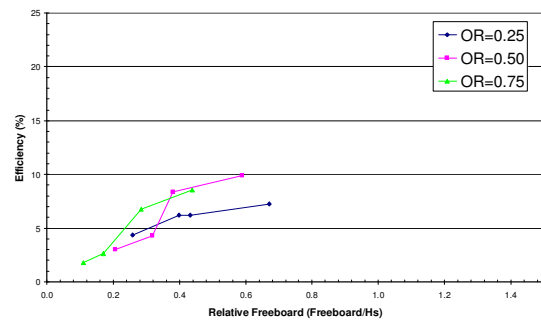
The results of the tests were made dimensionless using Eq. 3 where  $R$  is relative freeboard,  $R_c$  is crest freeboard and  $H_s$  is the measured significant wave height. Efficiency curves are displayed per wave period with respect to efficiency and relative freeboard in Figure 10.

$$R = \frac{R_c}{H_s} \quad (3)$$



(a). T<sub>p</sub>=1 s

Figure 10 (a)(b). Efficiency vs. relative freeboard



(b). T<sub>p</sub>=2 s

### Conclusion Model Testing

The primary conclusion that can be made from model testing is regarding the choice of opening ratio. Figure 10(a) shows that OR=0.75 performed less well than the other two ramps and that OR=0.50 has a higher peak efficiency while OR=0.25 has a wider range. The differences in Figure 10(b) are less significant and no clear conclusion can be made.

It should be noted that it became apparent from the results that a higher crest freeboard (OR=0.25) was advantageous considering the increase in storage capacity and reduction of spillback. Additionally, OR=0.25 experienced the most constant discharge of water while the other ramps experienced sporadic



and frequent negative discharge. Both high crest freeboard and constant discharge are beneficial characteristics for turbine efficiency.  $OR=0.25$  showed to be a more appropriate selection when periods of higher than expected overtopping (i.e. due to variability in wave conditions, tide or sea level rise) occur.

$OR=0.25$  has been selected as the most optimum opening ratio. As a result, a device efficiency curve has been generated as shown in Figure 11, where the data has been slightly modified to present a more realistic curve.

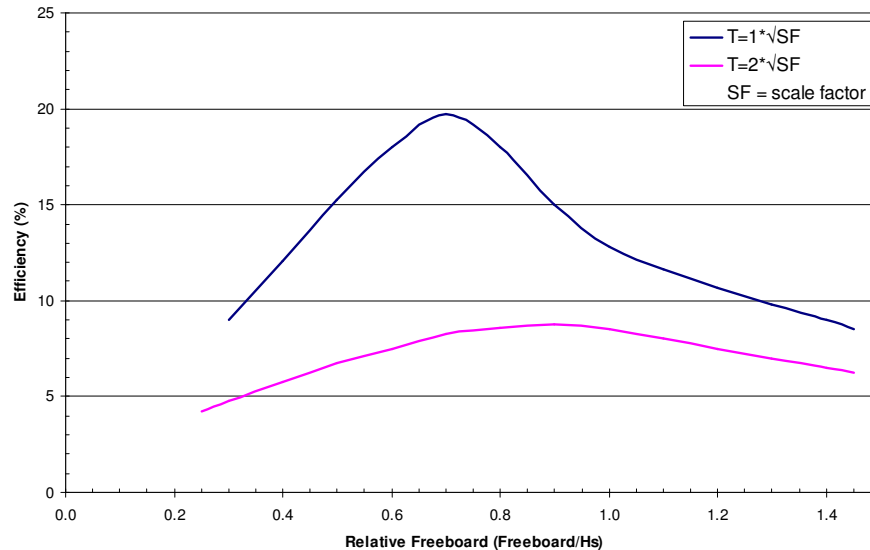


Figure 11. Device efficiency curve (Opening Ratio 0.25)

In order to use the efficiency curve, the scale factor selected for the full-scale design must be accounted for. Wave period is adjusted by the square root of the scale factor. Wave height and all full-scale dimensions have a linear relationship with the scale factor.

### SAMPLE LOCATIONS

Two locations were analysed for their potential energy production to gain insight into the effectiveness of the WEC. The locations were chosen based on several criteria:

- Wave climate similar to starting points wave climate
- Minimal tidal range
- Presence of existing breakwaters

Ultimately the locations Colón (Panama) and Sado (Japan) were selected. Although many locations met the criteria of site selection, these locations were specifically selected because of the differing wave climates. Panama had a highly unidirectional wave climate and Japan experienced large wave scatter.

### Calculation Simplification

Because this report is a proof of concept and not yet a full scale development, a few calculation simplifications were made.

**Caisson design:** For the locations an identical caisson design was used based on the Goda caisson design formulas (Goda 2000). The aim was not to fully design a caisson with WEC but to analyse the effectiveness of the WEC portion. Therefore a water depth of 15 m and overall caisson dimension of  $B=20$  m and  $H=22$  m was used at both locations.

**Inclusion of waves:** This WEC is to be integrated into a caisson breakwater. Therefore, only waves approaching from the front of the structure will impact the electrical production of the device. Additionally, because the model testing was performed using waves approaching normal to the device, only the efficiency of the conversion of perpendicular waves can be accurately predicted. It is expected that as the angle from normal to the breakwater increases the pressure exerted by the waves will decrease as well as the efficiency of conversion. An indication can be given using Goda's equations; however, in order to be conservative it is assumed only waves approaching from  $\pm 15^\circ$  from normal to

the breakwater will contribute to the conversion. A diagram of included and excluded waves for the purpose of the calculation is shown in Figure 12.

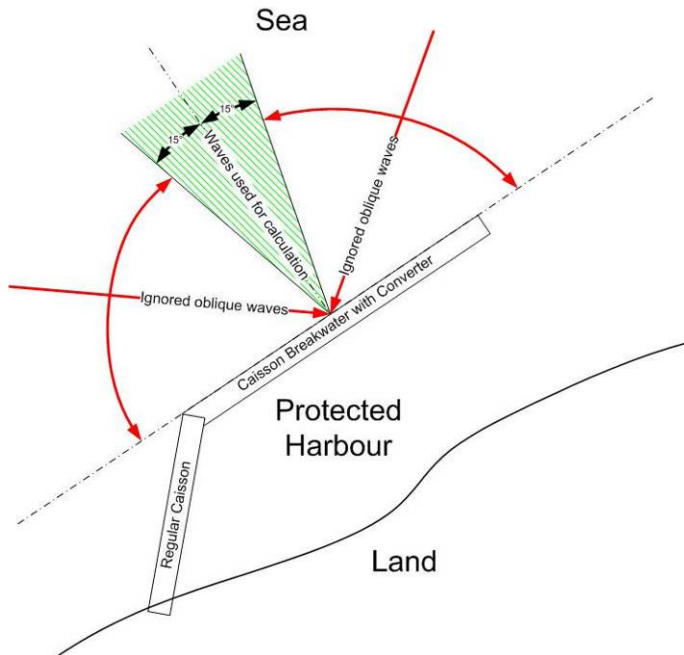


Figure 12. Inclusion/exclusion of incoming waves

**Tide:** Per location, mean high water spring and mean low water spring tidal information was collected from Admiralty Tidal Charts and used as maximum tidal range. It was assumed the maximum tidal range occurred purely sinusoidal which could be simplified to three tidal situations as described below and schematised as shown in Figure 13:

- Zero tide: No tide present
- Low tide: Average of 1/3rd lowest tidal levels
- High tide: Average of 1/3rd highest tidal levels

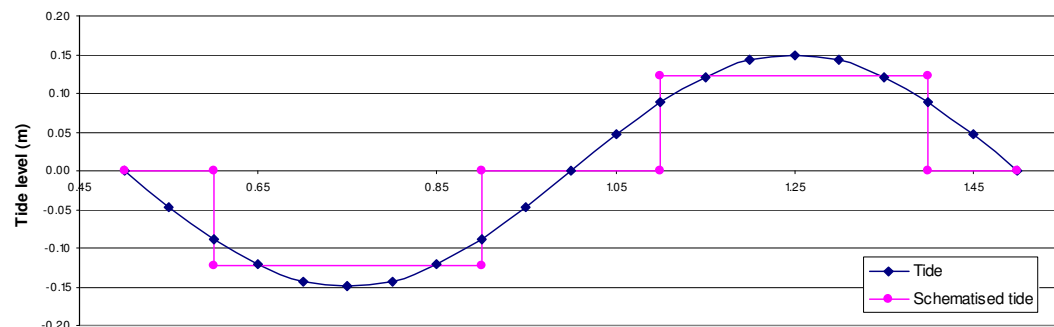


Figure 13. Tidal schematisation

The three simplified tidal situations were assumed to each occur 1/3rd of the time.

#### Calculation Procedure

The purpose of this calculation is to discover the optimum crest freeboard and the resulting possible electricity generation. A flowchart of the calculation procedure is presented in Figure 14.



4. Correct for expected system headloss for each tidal situation:

A certain headloss will be present in the system due to the fact that the elevation of the water in the basin will not be at the same elevation as the crest freeboard at all times. Therefore, it is assumed that the basin water elevation can always be kept above a certain level. Although the hydraulic head also becomes higher than this level, it is conservatively assumed it is always at the lowest level.

$\eta_{eff}$  is the effective efficiency that can be calculated using Eq. 4 where  $\eta$  is the efficiency from the previous calculation step,  $R_c$  is the crest freeboard, and  $h_L$  is the expected headloss in the system (assumed 20 cm).

$$\eta_{eff} = \frac{R_c - h_L}{R_c} \cdot \eta \quad (4)$$

5. Average resulting efficiency:

The effective efficiency (per tidal situation) is averaged and the resulting efficiency per wave condition,  $\eta_{avg}$ , is known.

6. Calculate resulting theoretical power generation per wave condition:

For wave conditions where an efficiency could be determined (see Table 6) Eq. 5 is used to calculate the theoretical power generation per wave condition ( $W_{wc}$ ) where  $W_{cap}$  is the capturable energy,  $W_{wave}$  is the calculated power per wave condition (Holthuijsen 2007) and  $P_{wave}$  is the wave condition probability of occurrence.

$$\begin{aligned} W_{wc} &= W_{cap} \cdot P_{wave} \\ W_{cap} &= \eta_{avg} \cdot W_{wave} \end{aligned} \quad (5)$$

It should be noted that, although the efficiency of energy conversion cannot be quantified for larger wave heights in the range  $T_p = 6 - 12$  s (in the case of the example in Table 6,  $H_s > 2.25$  m), it can be expected that at least as much energy can be converted for the larger wave heights. Therefore, for these larger wave heights  $W_{cap}$  will be equivalent to  $W_{cap}$  of the highest significant wave height with quantifiable efficiency.

7. Total power generation:

To calculate the total power generation a summation is made of all the theoretical power generation per wave condition multiplied by turbine efficiency (see Eq. 6).

$$W = \eta_T \cdot \sum W_{wc} \quad (6)$$

## WEC Design

The calculation procedure is repeated for several crest freeboard elevations in order to establish an optimum crest freeboard (in the case of no sea level rise). Sea level rise (SLR) can be accounted for by setting a higher crest freeboard and optimising the device output over the design lifetime. For the preliminary design of the two locations a design lifetime of 50 years was accounted for resulting in a 40 cm rise (linear rise of 80 cm per 100 years). Typical site wave climate characteristics are presented in Table 7. For a scale factor of 37.5 the model tested range is  $H_s = 0.75 - 2.25$  m and  $T_p = 6 - 12$  s.

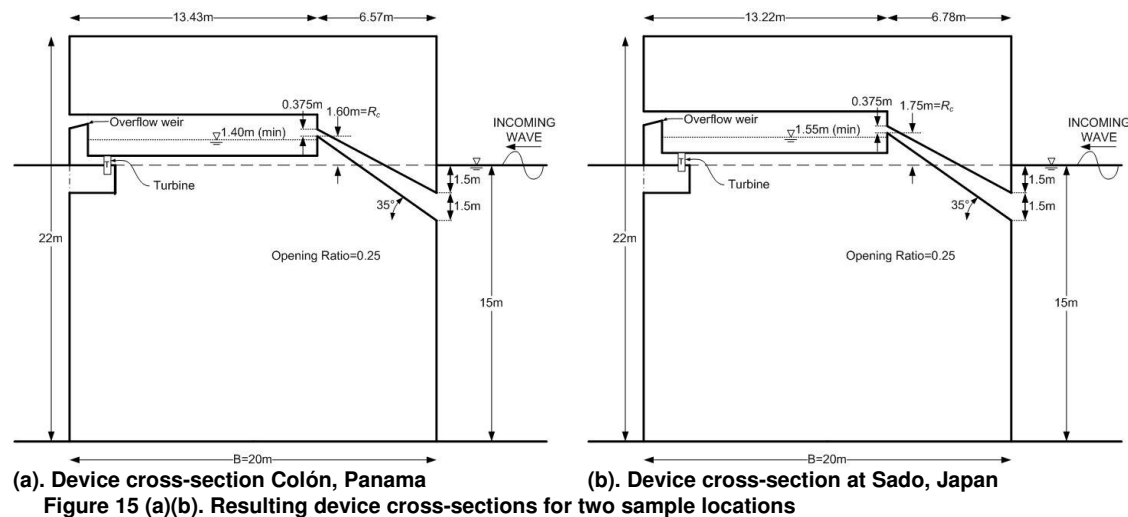
**Table 7. Characteristics of wave climate SF=37.5**

Location	Max. tide	Waves in 30° range (Figure 12)	Wave power in 30° range	Waves in model tested range
	[m]	[%]*	[kW/m <sup>1</sup> ]	[%]*
Colón, Panama	0.30	90.27	20.36	65.32
Sado, Japan	0.30	21.64	7.44	8.62

\* percent of total wave climate

Table 8 displays the results of the optimal crest freeboard and Figure 15 presents the resulting cross-sections for the two sample locations. The generic caisson dimensions were used.

<b>Table 8. Optimal crest freeboard</b>			
Location	Excluding SLR [m +MWL]	Including SLR (30 yr) [m +MWL]	Including SLR (50 yr) [m +MWL]
Colón, Panama	1.45	1.50	1.60
Sado, Japan	1.60	1.65	1.75



### Production Results

Based on the calculation procedure and the optimal crest freeboard in Table 8 the potential electrical production is calculated. The results are displayed in Table 9.

<b>Table 9. Electrical production results</b>			
Location	Excluding SLR [kWh/m <sup>1</sup> /yr]	Including SLR (30 yr) [kWh/m <sup>1</sup> /yr]	Including SLR (50 yr) [kWh/m <sup>1</sup> /yr]
Colón, Panama	16,656	16,522 (avg)	16,413 (avg)
Sado, Japan	5,855	5,826 (avg)	5,766 (avg)

Industrial electricity prices were found to be 0.104 and 0.117 USD/kWh in Panama and Japan, respectively (Energy information Administration 2008). Conservatively assuming these prices do not fluctuate over the lifetime of the structures allows for an estimate of the revenue or cost savings due to the production of electricity (Table 10).

<b>Table 10. Value of electricity produced</b>			
Location	Excluding SLR [USD/m <sup>1</sup> /yr]	Including SLR (30 yr) [USD/m <sup>1</sup> /yr]	Including SLR (50 yr) [USD/m <sup>1</sup> /yr]
Colón, Panama	\$1,732	\$1,718 (avg)	\$1,707 (avg)
Sado, Japan	\$685	\$682 (avg)	\$675 (avg)

It is interesting to note from Table 9 and Table 10 that the impact of SLR (over 50 years) is approximately 1.5 % compared to a situation of no SLR. However, the value of sea level rise should be accurately predicted. The difference in power output between the two locations can be attributed to the differing wave climates ( $H_s$ ,  $T_p$  and wave direction).

## RECOMMENDATIONS

### Optimisation

As this work was a proof of concept, there are many optimisations possible in order to increase the efficiency of the device.

**Storage basin:** The inclusion of a storage basin is important to ensure the turbines remain fully operational. Significant changes in hydraulic head and start/stop cycles will decrease the efficiency of energy conversion. Therefore, an opening ratio of 0.25 was selected which showed rather consistent discharge from the model. However, the water level within the basin will still fluctuate with every overtopping wave. The storage basin should be designed (together with turbine selection) to store an appropriate volume of water.

**Reducing losses:** Reducing losses present during the transformation of kinetic wave energy into potential energy is important. The first change that can be made is to introduce a rounded ramp entrance and exit. This will reduce the minor losses currently present due to the sudden shape change at the ramp entrance and exit. Designing the ramp to be short and ensuring a smooth concrete finish will reduce the headloss due to friction.

**Decreasing spillback:** It is believed a significant amount of energy may be lost through spillback. A feature should be designed to prevent or reduce the spillback observed during model testing. For example, as mentioned for Figure 7, energy dissipating elements were placed in the basin to reduce the waves from continued propagation through the internal basin.

**Increasing pressure:** Currently the vertical front portion of the caisson above the ramp entrance is flat. Possibly a trapezoidal shape can be added here to enhance the pressure exerted on the opening and therefore increase the volume of overtopping water.

### Future Work

In addition to increasing the efficiency of the WEC through optimisation the following refinements of model testing and calculation can be performed.

**Additional testing:** When calculating the power output of the two sample locations the usefulness of additional model testing data became apparent. More crest freeboards should be tested as well as additional wave climates. This will ensure the device efficiency curve (Figure 11) will be populated with plentiful data and will have a more clearly defined curve. Likewise, a more accurate calculation can be performed when finding the efficiency of the device at a particular location.

**Include oblique waves:** The effect of non-perpendicular waves on efficiency should be tested. Alternatively, Goda's wave pressure equations can be used to estimate the decrease in pressure reduction. Because only perpendicular waves were tested, the location analysis was conservative in only accounting for waves approaching from  $\pm 15^\circ$ . The remaining  $150^\circ$  of waves approaching the front of the caisson can still yield power production although likely at lower efficiency. It is expected that testing the efficiency level of these oblique waves will increase the overall efficiency of the device.

**Turbine selection:** Currently, a constant efficiency of 90 % is assumed for the turbine. A more exact value should be established by selecting an appropriate turbine. Care should be taken as the number of turbines suitable for this low head application may be limited. In addition to the type and size of turbine, the spacing of the turbine should be determined. The turbines should be spaced and sized such that the water elevation inside of the device will generally never drop more than 20 cm below the crest.

It is anticipated the device will use a system of several smaller turbines that can be remotely enabled and disabled, adjusting to the available flow of water. During periods of large overtopping all of the turbines will generate electricity while during periods of lesser overtopping only a few turbines will be activated.

**Opening ratio investigation:** During this research the main device characteristic that was determined was the optimum opening ratio. Three ratios were tested; however, it is possible that the most optimum opening ratio lies between the ones tested or that the optimum changes per wave climate.

**Vary additional parameters:** Interesting results may also be produced by varying the width of the ramps (spacing of internal walls) and ramp slopes. Additional research should also be performed on the effect of increasing the height of the ramp opening. Increasing the opening height will increase the pressure in the system because more of the dynamic wave load acts on the opening.



## CONCLUSION

The device that is proposed adequately complies with the starting points of the research. The device is shown to function properly in the specified wave climate while minimising the number of moving components. Combined with integration in a caisson breakwater the robustness of the WEC can be more easily and cost effectively ensured.

Integration in a breakwater as a fixed structure also creates limitations. The WEC would be most efficient if it could fluctuate with tide and sea level rise. The crest freeboard cannot change with the varying sea water elevation and therefore the crest freeboard cannot always be at the optimum height. Fortunately, it is seen that these negative effects can be managed by designing the WEC with a crest freeboard at an elevation that optimises the overall output.

Ultimately, this design has an overall average efficiency between approximately 9 and 12 %, measured as the percentage of wave climate energy converted to electricity over the device lifetime. However, it should be noted that all calculations and analysis were performed conservatively. Also, as the current research is a proof of concept, improvements in efficiency are possible by optimising device parameters. It is expected the overall average efficiency of the device will experience large gains through more precise calculation and design optimisation.

## Advantages

Despite the relatively low efficiency at the present development stage, this device has many advantages. Robustness is ensured through integration in a breakwater and by keeping the only moving component, the turbine, out of direct contact with wave action.

Another advantage is in terms of finances. Cost sharing is possible by integrating the device in a breakwater which will be built regardless of the inclusion of a WEC. With this device it is possible to marginally increase the construction cost of a breakwater while adding a secondary revenue generation function for the breakwater. It is only necessary for the revenue to offset the cost of the WEC portion of the structure.

Additionally, because energy is extracted from the incoming waves, the reflection coefficient of a caisson breakwater can be reduced. Vertical face breakwaters are generally attributed with a reflection coefficient of  $\pm 1.00$ . During model testing the reflection coefficient was reduced to  $\pm 0.50$ - $0.85$  depending on wave characteristics. Due to this reduction the overall breakwater dimensions may be reduced creating a more economically desirable breakwater design.

## ACKNOWLEDGMENTS

This paper presents the culmination of research work performed by the author as a master's thesis through the cooperation of Delft University of Technology and Delta Marine Consultants. Funding, support and wave flume access was provided by Delta Marine Consultants. Witteveen+Bos deserves special recognition for providing additional funding and support after the completion of the research.

## REFERENCES

- Energy Information Administration. 18 August 2008. Electricity Prices for Industry, <http://www.eia.doe.gov/emeu/international/elecprti.html>, Accessed July 2009.
- Goda, Y. 2000. Random Seas and Design of Maritime Structures, *World Scientific*, Singapore, 134-147.
- Holthuijsen, L.H. 2007. Waves in Oceanic and Coastal Waters, *Cambridge University Press*, Cambridge.
- Schoolderman, J.E. 2009. Generating electricity from waves at a breakwater in a moderate wave climate, *Delft University of Technology*, Delft.